

Supporting Information

Improve Efficiency and Stability of Pb-Sn Binary Perovskite Solar Cells by Cs Substitution

Xiao Liu^{1,2†}, Zhibin Yang^{1†}, Chu-Chen Chueh¹, Adharsh Rajagopal¹, Spencer T. Williams¹, Ye Sun² and Alex K.-Y. Jen^{1,}*

¹X. Liu, Dr. Z. Yang, Dr. C.-C. Chueh, S. T. Williams, A. Rajagopal and Prof. A. K.-Y. Jen
Department of Materials Science and Engineering, University of Washington, Seattle, WA,
98195-2120, USA

²Condensed Matter Science and Technology Institute, School of Science, Harbin Institute of
Technology, Harbin 150080, China

*Corresponding author. E-mail: ajen@u.washington.edu

† These two authors contribute equally to this work

Keywords: Cs substitution, Pb-Sn alloy perovskite, Compositional engineering, Stability

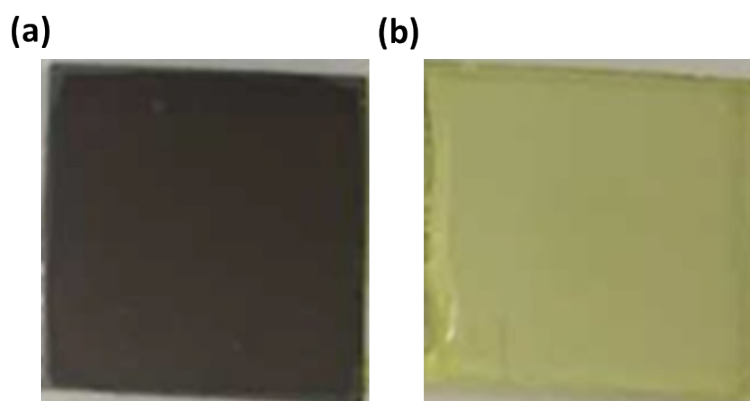


Figure S1. MASnI₃ (a) and CsSnI₃ (b) perovskite films after toluene washing process before annealing.

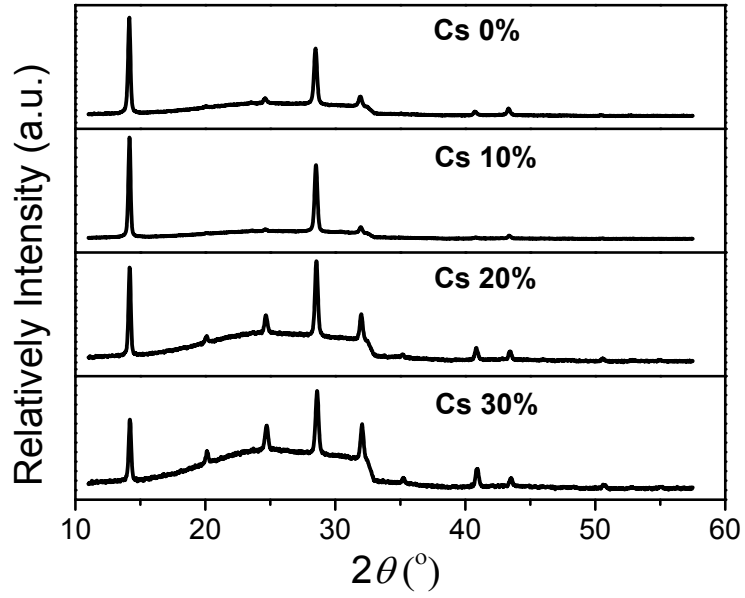


Figure S2. Refined XRD spectra of $\text{MA}_{1-y}\text{Cs}_y\text{Pb}_{0.5}\text{Sn}_{0.5}\text{I}_3$.

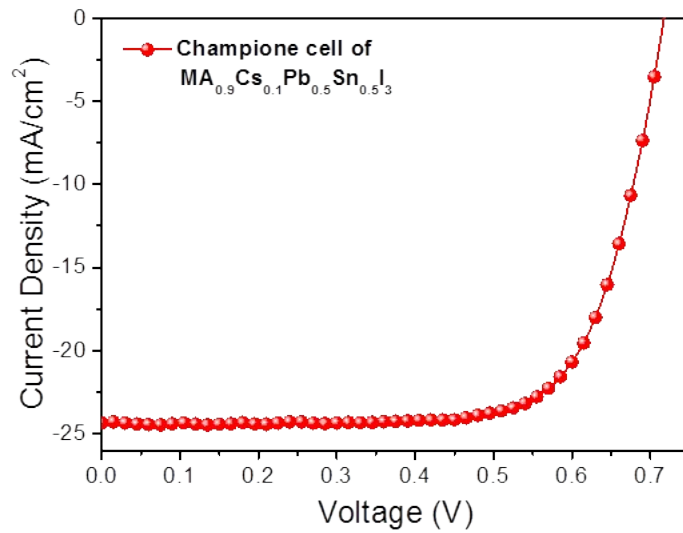


Figure S3. J - V curve of the champion device based on $\text{MA}_{0.9}\text{Cs}_{0.1}\text{Pb}_{0.5}\text{Sn}_{0.5}\text{I}_3$ perovskite measured under AM 1.5 illumination under reverse scan.

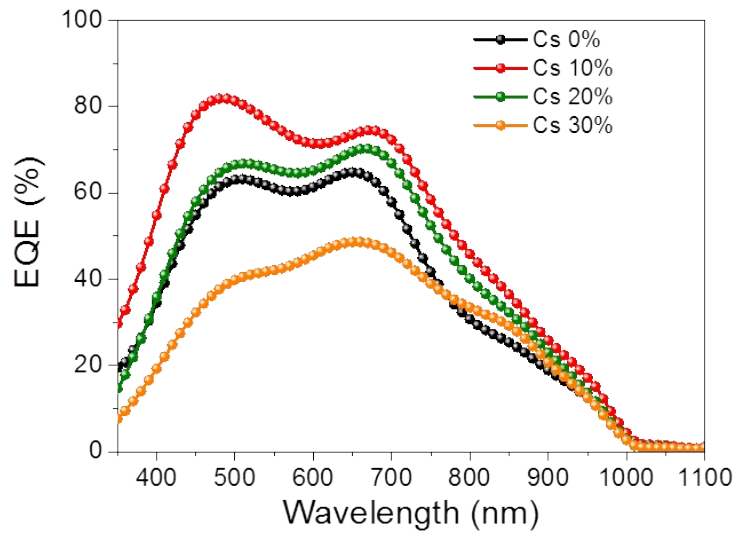


Figure S4. EQE of $\text{MA}_{1-x}\text{Cs}_x\text{Pb}_{0.5}\text{Sn}_{0.5}\text{I}_3$ ($x=0, 0.1, 0.2, 0.3$) PVSCs.

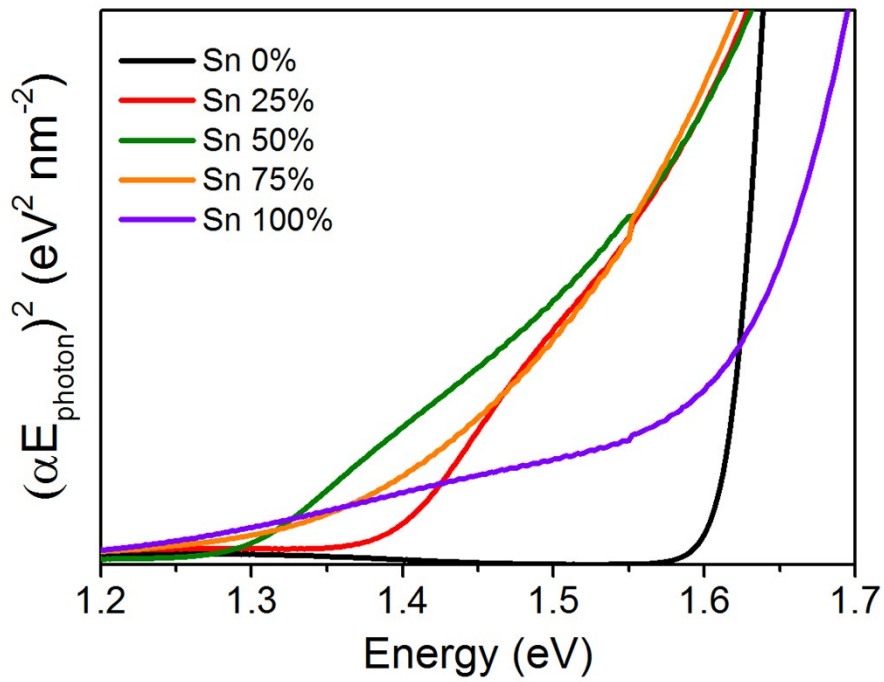


Figure S5. Tauc-plot analysis of $\text{MA}_{0.9}\text{Cs}_{0.1}\text{Pb}_{1-x}\text{Sn}_x\text{I}_3$ ($x=0, 0.25, 0.5, 0.75, 1$) perovskite films.

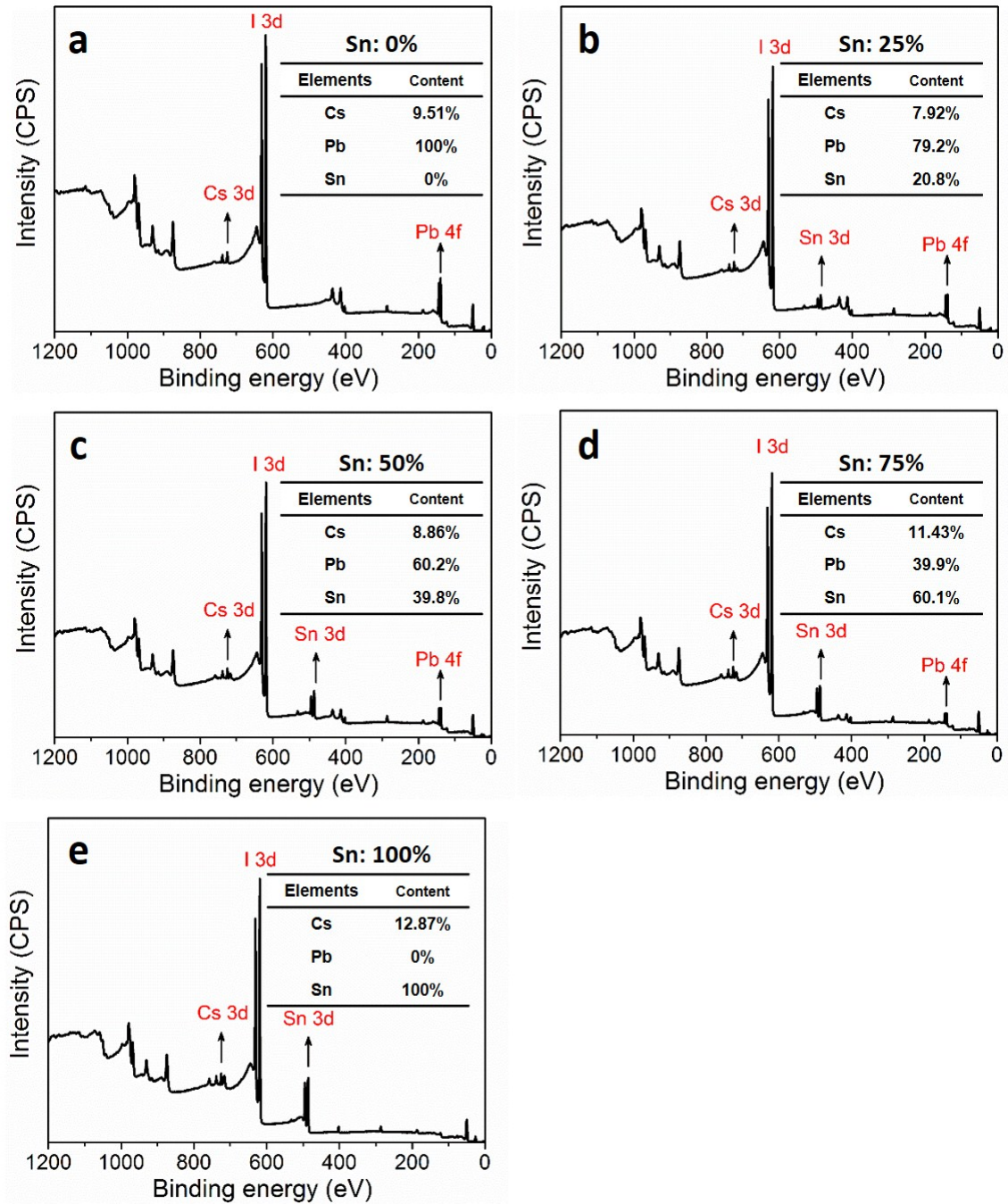


Figure S6. XPS analysis of $\text{MA}_{0.9}\text{Cs}_{0.1}\text{Pb}_{1-x}\text{Sn}_x\text{I}_3$ ($x=0, 0.25, 0.5, 0.75, 1$) films.

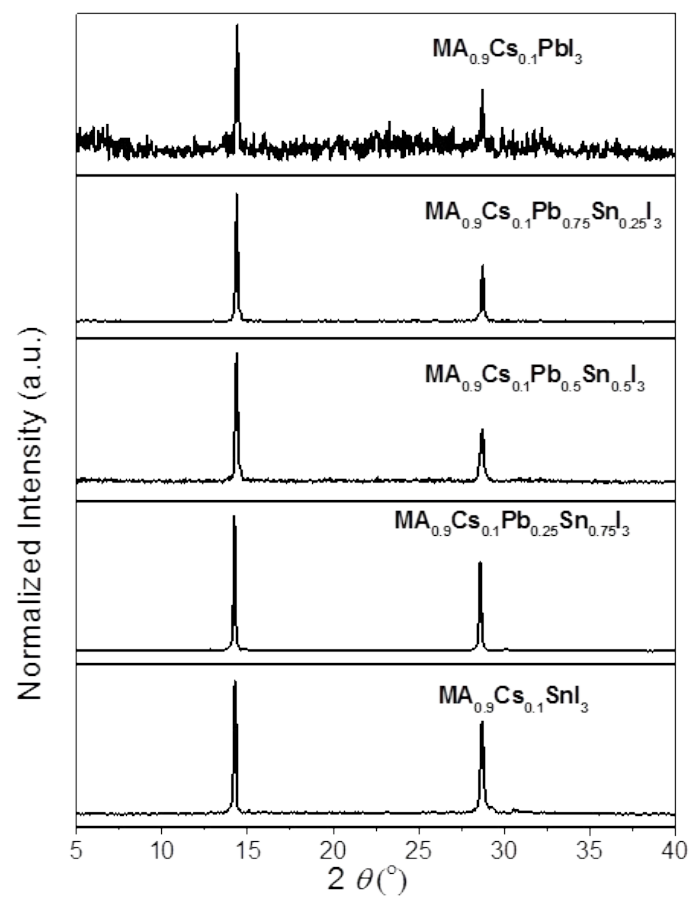


Figure S7. XRD spectra of MA_{0.9}Cs_{0.1}Pb_{1-x}Sn_xI₃ (x=0, 0.25, 0.5, 0.75, 1) films.

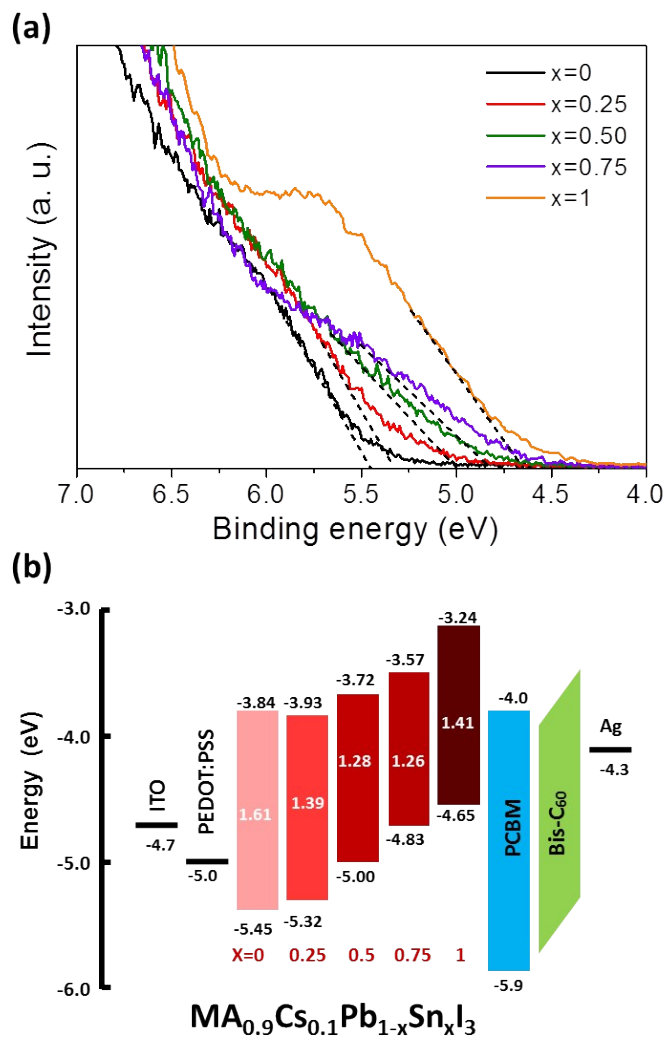


Figure S8. (a) UPS and (b) the corresponding energy diagram of MA_{0.9}Cs_{0.1}Pb_{1-x}Sn_xI₃ (x=0, 0.25, 0.5, 0.75, 1) films.

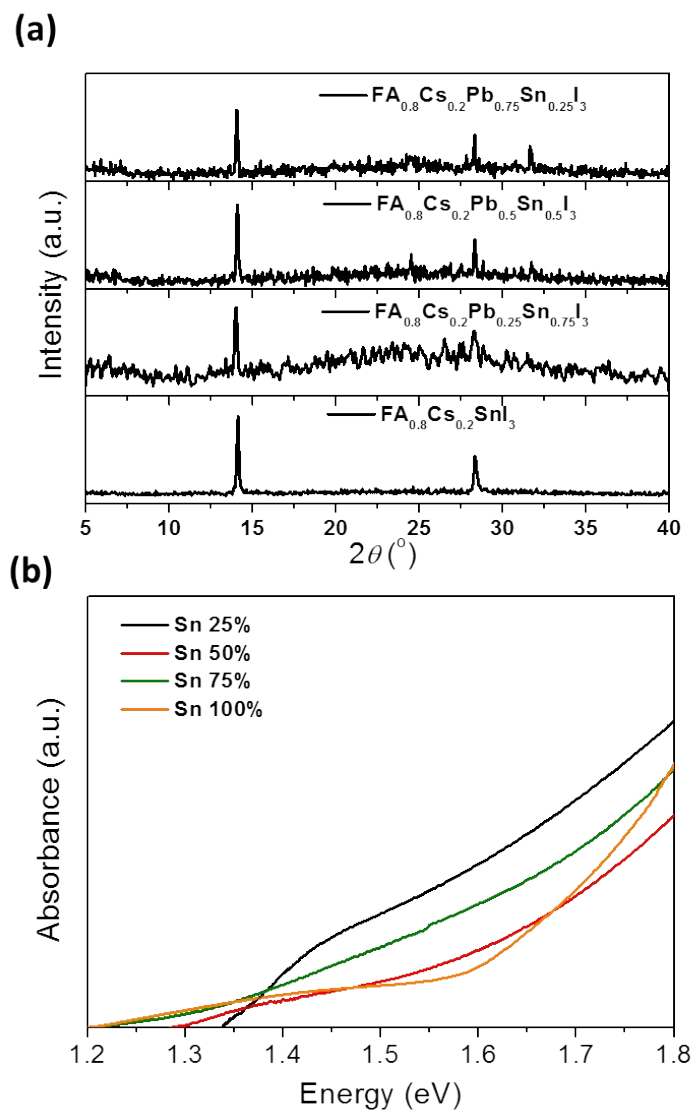


Figure S9. (a) XRD and (b) UV-Vis spectra of $\text{FA}_{0.8}\text{Cs}_{0.2}\text{Pb}_{1-x}\text{Sn}_x\text{I}_3$ ($x=0.25, 0.5, 0.75, 1$) films.

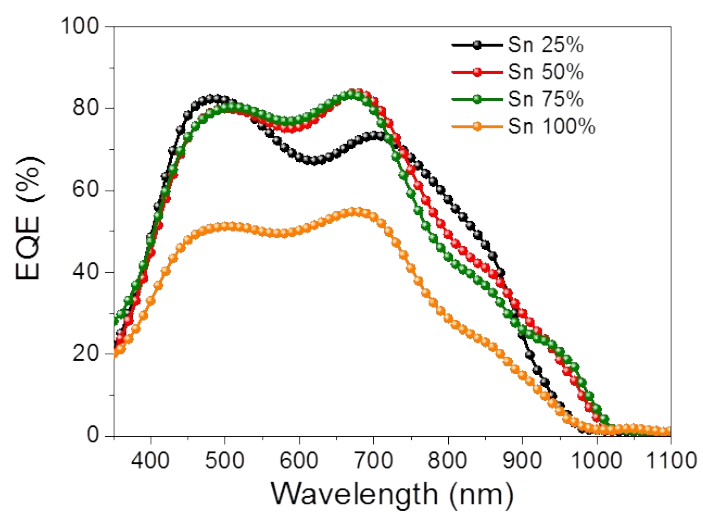


Figure S10. EQE of $\text{FA}_{0.8}\text{Cs}_{0.2}\text{Pb}_{1-x}\text{Sn}_x\text{I}_3$ ($x=0.25, 0.5, 0.75, 1$) PVSCs.

Table S1. Lattice parameters and volume of MA_{1-x}Cs_xPb_{0.5}Sn_{0.5}I₃ (x=0, 0.1, 0.2, 0.3)

Crystal Lattice	<i>a</i> (Å)	<i>c</i> (Å)	Volume (Å ³)
MAPb _{0.5} Sn _{0.5} I ₃	8.85	12.53	981.4
MA _{0.9} Cs _{0.1} Pb _{0.5} Sn _{0.5} I ₃	8.84	12.54	979.7
MA _{0.8} Cs _{0.2} Pb _{0.5} Sn _{0.5} I ₃	8.83	12.49	973.3
MA _{0.7} Cs _{0.3} Pb _{0.5} Sn _{0.5} I ₃	8.81	12.46	968.6

Table S2. Performance of MA_{1-x}Cs_xPb_{0.5}Sn_{0.5}I₃ (x=0, 0.1, 0.2, 0.3) PVSCs measured under AM 1.5 illumination under reverse scan.

Composition	<i>V</i> _{oc} (V)	<i>J</i> _{sc} (mA/cm ²)	FF (%)	PCE (%)
MAPb _{0.5} Sn _{0.5} I ₃	0.62	18.65	55.0%	6.36
MA _{0.9} Cs _{0.1} Pb _{0.5} Sn _{0.5} I ₃	0.70	23.32	61.7%	10.07
MA _{0.8} Cs _{0.2} Pb _{0.5} Sn _{0.5} I ₃	0.60	20.58	60.7%	7.50
MA _{0.7} Cs _{0.3} Pb _{0.5} Sn _{0.5} I ₃	0.39	14.96	50.4%	2.94

Table S3. Performance of FAPb_{1-x}Sn_xI₃ and FA_{0.8}Cs_{0.2}Pb_{1-x}Sn_xI₃ (x=0.25, 0.5, 0.75, 1) PVSCs measured under AM 1.5 illumination with reverse scan.

Composition	<i>V</i> _{oc} (V)	<i>J</i> _{sc} (mA/cm ²)	FF (%)	PCE (%)
FAPb _{0.75} Sn _{0.25} I ₃	0.75	19.48	70.3%	10.27
FAPb _{0.5} Sn _{0.5} I ₃	0.60	21.52	65.4%	8.44
FAPb _{0.25} Sn _{0.75} I ₃	0.46	20.43	56.1%	5.27
FASnI ₃	0.04	11.73	23.4%	0.11
FA _{0.8} Cs _{0.2} Pb _{0.75} Sn _{0.25} I ₃	0.84	22.73	75.7%	14.46
FA _{0.8} Cs _{0.2} Pb _{0.5} Sn _{0.5} I ₃	0.70	24.30	68.3%	11.63
FA _{0.8} Cs _{0.2} Pb _{0.25} Sn _{0.75} I ₃	0.56	24.44	57.2%	7.83
FA _{0.8} Cs _{0.2} SnI ₃	0.24	16.05	35.8%	1.38